JOURNAL OF MATERIALS SCIENCE 32 (1997) 1039–1047

Effects of thermal cycling on thermal expansion and mechanical properties of SiC fibre-reinforced reaction-bonded Si_3N_4 composites

R.T. BHATT, A.R. PALCZER
NASA Lewis Research Center, Cleveland, OH 44135, USA

Thermal expansion curves for SiC fibre-reinforced reaction-bonded Si_3N_4 matrix composites (SiC/RBSN) and unreinforced RBSN were measured from 25 to 1400 °C in nitrogen and in oxygen. The effects of fibre/matrix bonding and cycling on the thermal expansion curves and room-temperature tensile properties of unidirectional composites were determined. The measured thermal expansion curves were compared with those predicted from composite theory. Predicted thermal expansion curves parallel to the fibre direction were between the measured curves for the strongly- and weakly-bonded composites, but those normal to the fibre direction for both bonding cases were similar to that of the unreinforced RBSN. Thermal cycling in nitrogen for both bonding cases resulted in no net dimensional changes at room temperature and no loss in tensile properties from the as-fabricated condition. In contrast, thermal cycling in oxygen for both composites caused volume expansion primarily due to internal oxidation of RBSN. Cyclic oxidation affected the mechanical properties of the weakly-bonded SiC/RBSN composites the most, resulting in loss of strain capability beyond matrix fracture and catastrophic, brittle fracture. Increased bonding between the SiC fibre and RBSN matrix due to oxidation of the carbon-rich fibre surface coating and an altered residual stress pattern in the composite due to internal oxidation of the matrix are the main reasons for the poor mechanical performance of these composites.

1. Introduction

Fibre-reinforced ceramic matrix composites are being developed for high temperature heat engine components because these materials potentially offer the advantage of monolithic ceramic materials, namely, high strength and oxidation resistance, while also providing mechanisms for crack deflection at the fibre/matrix interface for improved strain capability and reliability. Incorporation of these materials in high-temperature applications requires mechanical and dimensional stability under severe thermal shock and thermal cycling conditions. A variety of fibre-reinforced ceramic matrix composites [1–5] are being developed which show promise for these applications. In most cases, the reinforcement fibres for these composites are chosen based on their thermal expansion and chemical compatibility with the matrix. To reduce the thermal residual stresses generated in the composite after cooling down from the fabrication temperature and during thermo-mechanical fatigue, the thermal expansion difference between the fibre and the matrix should be kept to a minimum. Even when this is the case, thermal residual stresses may be generated due to thermal gradients during cycling and fabrication related problems such as non-uniform matrix microstructure, non-uniform fibre distribution, or variation in fibre/matrix bonding. Therefore, for any potential high temperature structural composite, a basic understanding of the effects of thermal cycling on thermal expansion and mechanical properties is necessary in order to evaluate and improve its thermomechanical behaviour. The objectives of this study were three-fold. The first objective was to evaluate the effects of thermal cycling on a SiC fibre reinforced reaction-bonded Si_3N_4 matrix (SiC/RBSN) composite system. The advantages of this composite for engine applications have been discussed elsewhere [6]. Changes in thermal expansion and in residual mechanical properties were used to evaluate the cycling effects for unidirectional composites. A second objective was to determine the applicability of current composite theory in predicting the observed thermal expansion behaviour. A third objective was to determine the influence of fibre/matrix bonding on thermal expansion and room-temperature properties of the unidirectional SiC/RBSN composite.

2. Experimental procedure

For SiC/RBSN composite fabrication, SiC fibres of average diameter 142 μm and high-purity silicon powder of average particle size 0.6 μm were used. Two types of SiC fibres, designated by the manufacturer as SCS-0 and SCS-6, were obtained from Textron

0022–2461

Specialty Materials. Both fibres were made by a chemical vapour deposition (CVD) technique in which SiC is deposited onto to a 37 μm diameter carbon core. Except for the surface coating, both fibres had identical microstructures. The SCS-0 fibres had no surface coating; the SCS-6 fibres had an approximately 3 μm thick SiC-containing carbon-rich coating on top of the SiC substrate. The carbon-coating consists of two distinct sublayers each of which contained a mixture of SiC particles and turbostratic carbon [7]. The size and concentration of SiC particles within each layer varied with the location.

The SiC/RBSN composites were fabricated by conventional ceramic powder processing methods using a fugitive polymer binder [8]. The composite fabrication involved four steps: fabrication of fibre mats; fabrication of silicon tapes; consolidation of a preform by warm pressing of alternate layers of fibre mat and silicon tape in a vacuum hot press; and finally nitridation of SiC/Si performs at appropriate conditions to convert the silicon to a silicon nitride matrix. Both unreinforced RBSN and unidirectional SiC/RBSN composite panels of two different thicknesses were fabricated. The composite panels contained either SCS-0 or SCS-6 fibres. Typical dimensions of the panels with two different thicknesses were 127 mm × 50 mm × 2.5 mm and 127 mm × 50 mm × 6.5 mm.

The as-fabricated nitrided panels were surface ground to remove surface irregularities and loose Si_3N_4 particles, and then cut with a diamond impregnated abrasive wheel. For the thermal expansion study, specimens of approximate dimensions 50 mm × 6 mm × 6 mm were cut from the thicker panels. Some of the composite specimens were cut such that the fibre direction was parallel to, and in others normal to, the 50 mm length.

Thermal expansion curves for the composite specimens both parallel and normal to the fibre directions, and unreinforced RBSN were measured using an automatic recording dilatometer (Netzsch Dilatometer, Model STA 429) in nitrogen (99.999% purity) and in dry oxygen (< 10 p.p.m. moisture) from 250 to 1400 °C while heating at 50 °C min^{-1}. Each specimen was cycled at least 5 times. The physical dimensions and weights of the specimens before and after cycling were measured.

For thermal cycling, specimens of dimensions 115 mm × 6 mm × 2.2 mm were also cut from the thinner panels. Each specimen was thermally cycled in an alumina tube furnace from 25 to 1400 °C in nitrogen or in oxygen at heating and cooling rates of 50 °C min^{-1}. The temperature was measured at the centre of the specimens using a thermocouple. After cycling, specimens were prepared for tensile testing. The procedure involved adhesively bonding glass fibre-reinforced tabs of dimensions 38 mm × 6 mm × 1 mm to both sides at each end of the specimen, leaving 39 mm as the gauge length. A wire wound strain gauge was adhesively bonded to the specimen at the central section of the gauge area to monitor axial strain. The specimens were tensile tested at room temperature at a constant crosshead speed of 5 mm min^{-1} in an universal tensile testing machine equipped with wedge grips. After each exposure condition, at least 5 specimens were tested.

3. Results and discussion

Physical properties and microstructure of the SCS-0/RBSN composites were similar to those of the SCS-6/RBSN composites. Each composite specimen contained ~ 24 vol % fibres and was ~ 70% dense. Representative cross-sections of both composites are shown in Fig. 1. Because the SCS-0 fibres have no surface coating, these fibres reacted with the matrix to form a strong bond under the fabrication conditions. A previous study [9] has reported an interfacial shear strength (ISS) of 200 MPa in this system. Because of its high ISS, this system is henceforth also referred to as the strongly-bonded system. In contrast, in the SCS-6/RBSN composites, the SCS-6 fibres did not significantly react with the matrix during processing because of the carbon-rich surface coating. These composites have a relatively low interfacial shear strength; typically 10 ± 5 MPa [2]. Therefore this system is also referred to as the weakly-bonded system in this paper.

3.1. Cycling effects in nitrogen

Typical heating and cooling dilatometer curves parallel and normal to the fibre directions for the

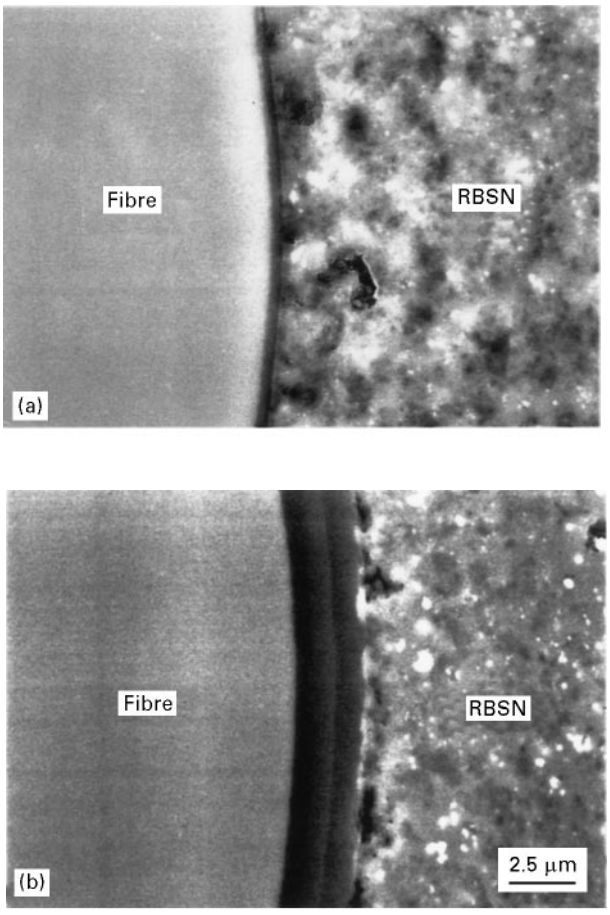

Figure 1 Cross-sections showing interface regions of two different SiC/RBSN composites; (a) SCS-0/RBSN and (b) SCS-6/RBSN.

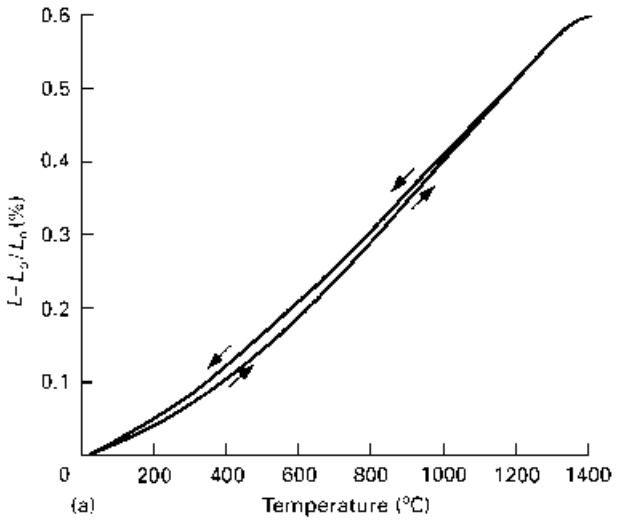

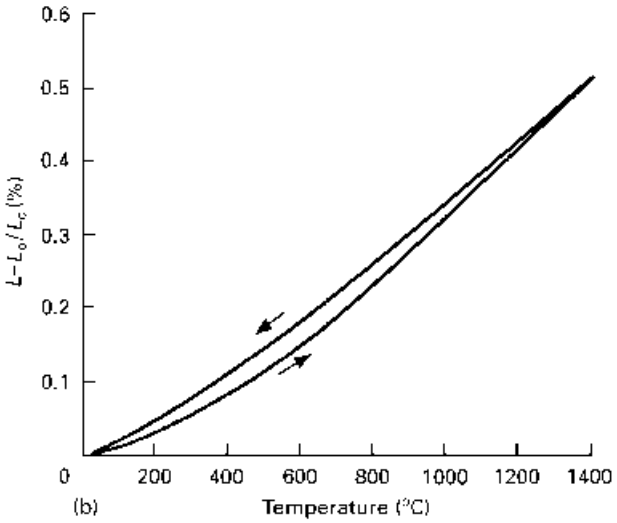

Figure 2 Thermal expansion curves for a SCS-0/RBSN composite ($V_f \sim 0.24$) in nitrogen; (a) parallel to the fibre and (b) normal to the fibre.

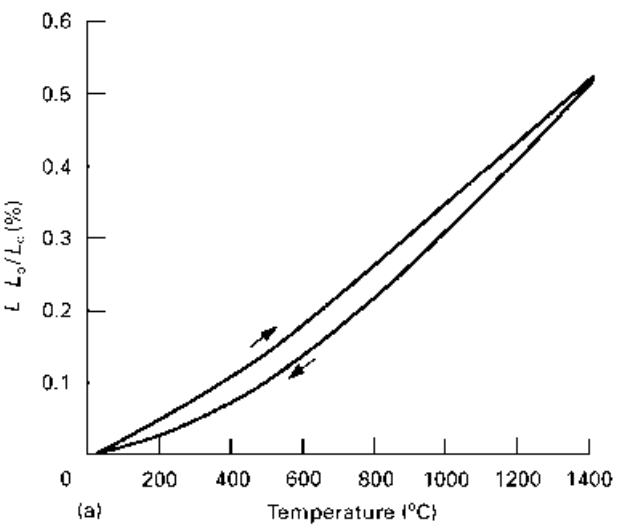

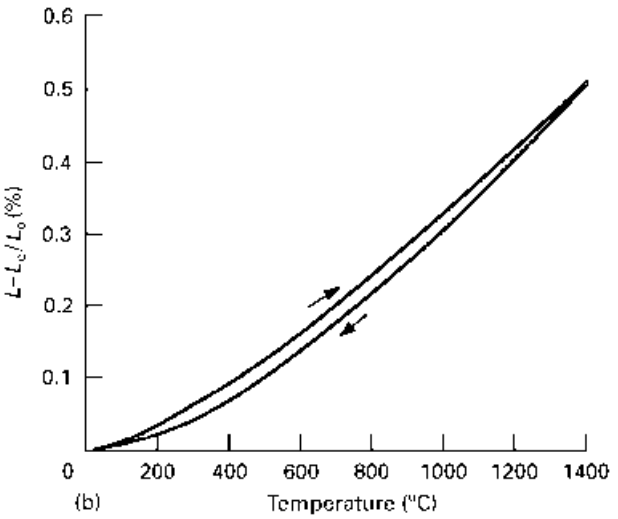

Figure 3 Thermal expansion curves for a SCS-6/RBSN composite ($V_f \sim 0.24$) in nitrogen; (a) parallel to the fibre and (b) normal to the fibre.

strongly-bonded SCS-0/RBSN and weakly-bonded SCS-6/RBSN composites cycled between 250 and 1400 °C in nitrogen are shown in Figs 2 and 3, respectively. Comparison of these two figures indicates several notable features. First, both heating and cooling curves were generally upwardly concave. Second, the SCS-6/RBSN composite displayed appreciably more hysteresis compared to the SCS-0/RBSN composites. Third, the thermal expansion curves normal to the fibre direction generally showed a greater amount of hysteresis than those parallel to the fibre. Fourth, at the same temperature, the thermal expansion for the SCS-0/RBSN composites during heating was lower than that during cooling, whereas for the SCS-6/RBSN composite the trend was opposite. Fifth, heating and cooling curves in the first and second cycle were slightly different, but after the second cycle, they were reproducible. Measurements of specimen length after each cycle indicated no length change, and specimen weight remained nearly the same with each cycle. The amount of hysteresis, as measured by the area bounded within the heating and cooling curves, also decreased with cycling which suggests microstructural adjustment within the material.

Thermal expansion curve of the strongly-bonded unidirectional composites can be reasonably predicted from two rule-of-mixtures models using constituent thermal expansion values and elastic properties. Two models are the Schapery model, which is based on energy principles [10], and the Turner model, which is based on stress-equilibrium [11]. Both models are nearly the same and each quantitatively accounts for the relative portions of the composite's components. The Turner model makes use of weight fraction and density as parameters, whereas the Schapery model uses the volume fraction. In the present study we used the Schapery model. According to this model, thermal expansions parallel, α_{11}, and normal, α_{22}, to the fibre direction are given by the equations,

$$\alpha_{11} = (E\alpha)/E$$

$$E\alpha = E_f \alpha_f V_f + E_m \alpha_m V_m$$

and

$$E = E_f V_f + E_m V_m$$

and

$$\alpha_{22} = \alpha_f V_f (1 + \gamma_f) + \alpha_m V_m (1 + \gamma_m) - [(\gamma_f V_f + \gamma_m V_m)(E\alpha)/E]$$

TABLE I Physical and elastic properties of SiC fibres and RBSN matrix

Material	E (GPa)	γ	Density ($g\,cc^{-1}$)
SCS-0 fibres	390 [a]	0.17 [b]	3.00 [a]
SCS-6 fibres	390 [a]	0.17 [b]	3.00 [a]
RBSN	110 [c]	0.22 [c]	1.92 [c]

[a] [12]
[b] [13]
[c] [2]

Here E is the elastic modulus, α is the thermal expansion coefficient, V is the volume fraction, γ is Poisson's ratio and the subscripts f and m refer to the fibre and the matrix, respectively.

Using the constitutive elastic properties from Table I, the thermal expansion data for the CVD SiC fibre along the fibre axis from [12] and the above equations, thermal expansion curves for the SiC/RBSN composites during heating were predicted. The thermal expansion data for SiC is assumed to be isotropic because the fibre is a cubic material. The measured and predicted thermal expansion curves for the strongly and weakly-bonded SiC/RBSN composites for the two orientations are shown in Fig. 4. Included in the figure is the measured thermal expansion trace of unreinforced RBSN for comparison. In the direction parallel to the fibre, the measured and predicted curves agreed well up to 700 °C. Beyond this temperature, the predicted curve is lower than the measured curve for the SCS-0/RBSN, but above the trace for the SCS-6/RBSN. In the direction normal to the fibre, the predicted and the measured curves for both composites agreed well and were similar to the measured curve for the unreinforced RBSN. This indicates that in this composite system, fibre/matrix bonding has a strong influence on the thermal expansion trace along the fibre direction and has weak influence on the thermal expansion curve in the direction normal to the fibre.

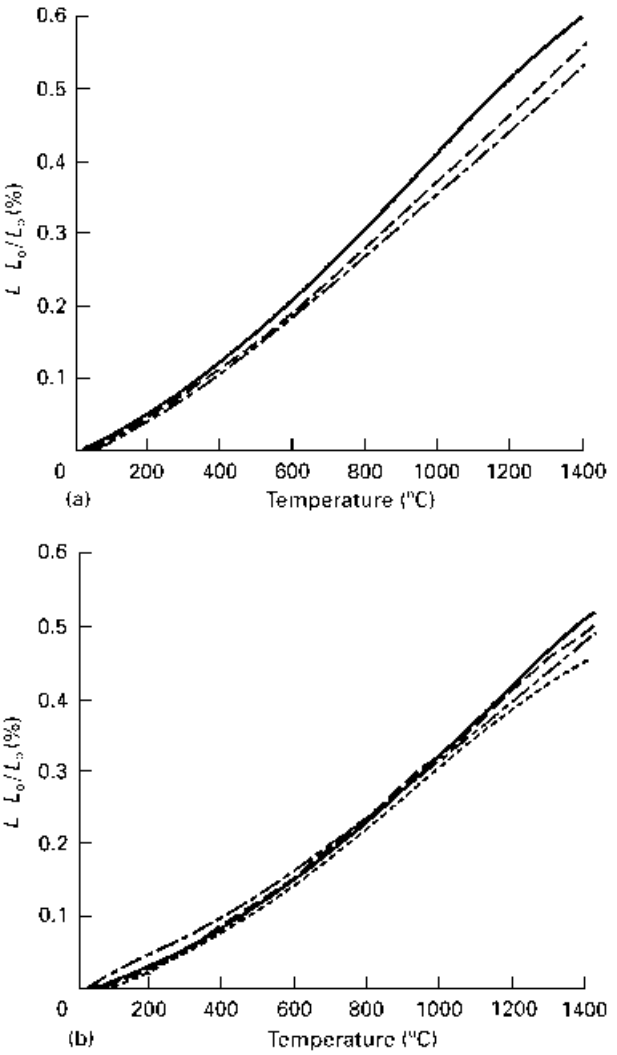

Figure 4 Measured and predicted thermal expansion curves for the SiC/RBSN composites in nitrogen; (a) parallel to the fibre and (b) normal to the fibre (— measured (SCS-0/RBSN); – – – predicted; —·— measured (SCS-6/RBSN); - - - - measured RBSN).

3.2. Cycling effects in oxygen

The effects of thermal cycling in oxygen on the heating and cooling curves of the SCS-0/RBSN and SCS-6/RBSN composites parallel and normal to the fibre direction are illustrated in Figs 5 and 6. Again both heating and cooling curves were non-linear; typically upwardly concave. Comparison of Figs 2 and 3, and Figs 5 and 6 shows that the thermal expansion curves of both composites cycled in oxygen display more hysteresis in the first few cycles than those cycled in nitrogen. At the end of the first cycle, i.e. at room temperature, the cooling curves of both composites showed a positive shift in $((L - L_0)/L_0)$; an indication of length increase. With each additional cycle, a further increase in specimen length was observed, but the rate of increase in length/cycle consistently decreased. Specimen weight also increased in the first two cycles and then reached a plateau which corresponded to a total weight gain of $\sim 3.5\%$. After the third cycle, reproducible thermal expansion curves with no apparent hysteresis were obtained, and no apparent difference in thermal expansion curves was noticed between the SCS-0/RBSN and SCS-6/RBSN composites, which suggests that after initial adjustment in the microstructures of components, the fibre/matrix bonding had little effect on the thermal expansion curve. Specimen length increases in composites can be due to phase transformation or oxidation of constituents. Since length increases were not observed in composites cycled in nitrogen, phase transformation may not be a factor. Under the cyclic conditions, there is no evidence of length change in SCS-6 fibres due to oxidation. Therefore environmental effects on the thermal expansion curve of unreinforced RBSN were investigated. The results, illustrated in Fig. 7, indicate, as expected, that thermal cycling in nitrogen had no appreciable effect on the thermal expansion curve or on specimen length, but thermal cycling in oxygen resulted in hysteresis, length extension, and weight gain similar to those for the composites. Per cent length increases observed per cycle in each composite and in the unreinforced RBSN are reported in Table II. In general, the unreinforced RBSN shows lower

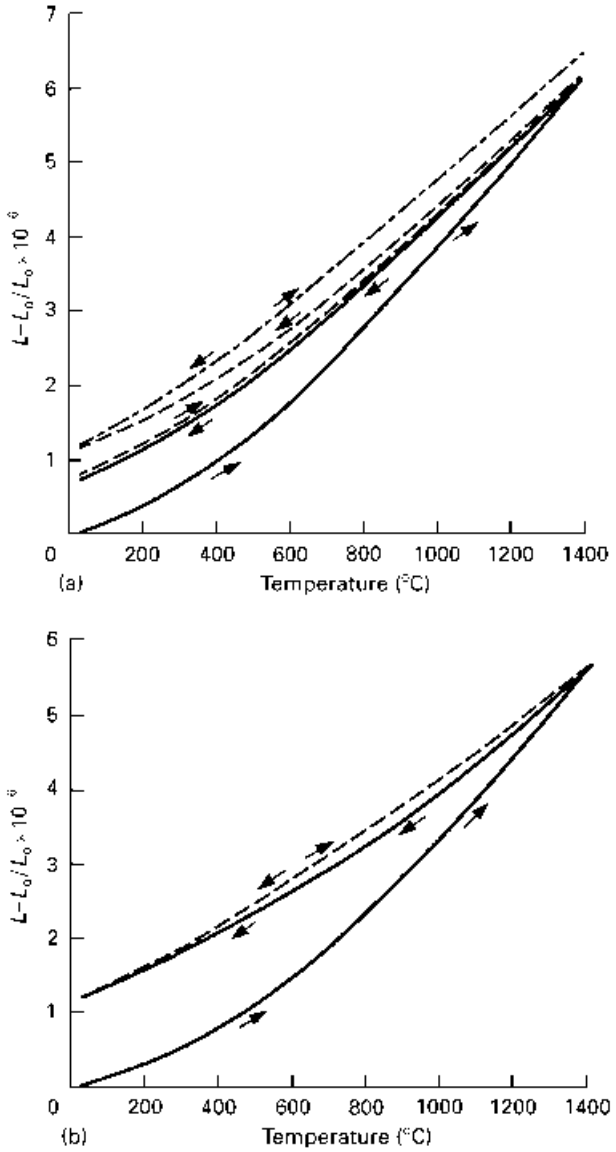

Figure 5 Effects of thermal cycling in oxygen on the thermal expansion curve of a SCS-0/RBSN composite ($V_f \sim 0.24$); (a) parallel to the fibre (—— 1st cycle; ———— 2nd cycle; – - – 3rd to 6th cycle) and (b) normal to the fibre (—— 1st cycle; – – – 2nd to 6th cycle).

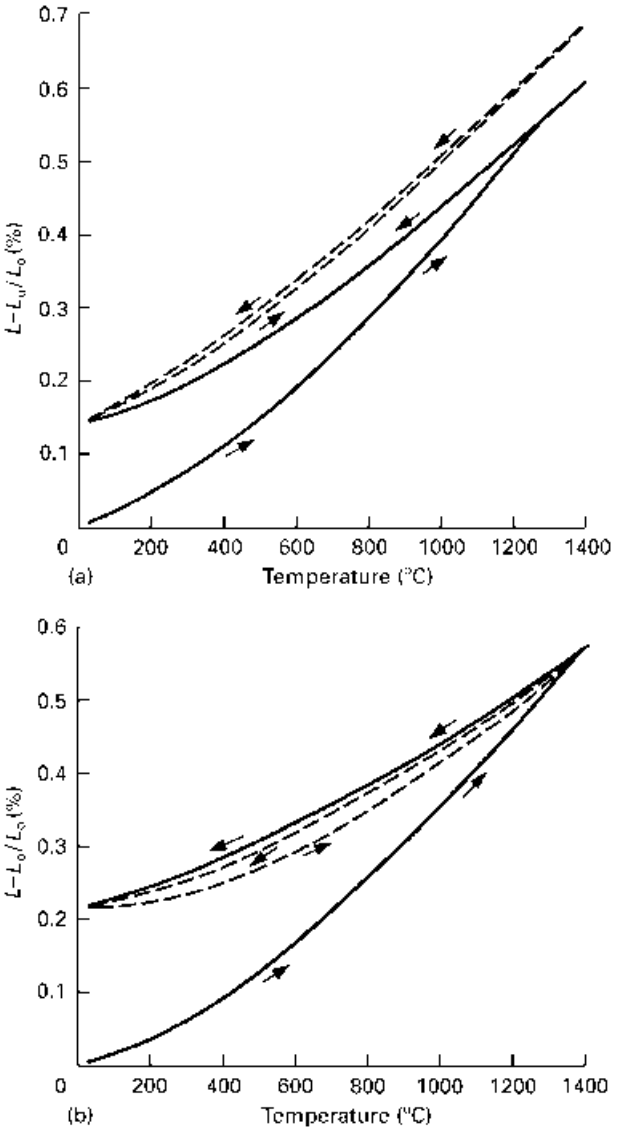

Figure 6 Effects of thermal cycling in oxygen on the thermal expansion curve of a SCS-6/RBSN composite ($V_f \sim 0.24$); (a) parallel to the fibre and (b) normal to the fibre (—— 1st cycle; – – – 2nd to 6th cycle).

length increase than the composite in the normal to the fibre direction. This difference can be the result of smaller average pore size seen in the unreinforced RBSN matrix compared with the composite.

Since RBSN is a porous material and most of the porosity is interconnected, exposing it to oxygen results in growth of silica on the geometrical surfaces and the surfaces of pores as well. However, the pore wall oxidation ends quickly with the sealing of the pore channels near the surface because of the 82% increase in volume during conversion of a mole of silicon nitride to a mole of silica. Beyond this stage, oxidation is limited to the geometrical surfaces, as shown in Fig. 8. During cycling the surface silica layer appears to have cracked normal to the substrate. Growth of silica on the pore walls as well as on the external surfaces accounts for length increase in the unreinforced RBSN and SiC/RBSN composites.

Studies [14, 15] have shown that internal oxidation of RBSN is severe between 900 to 1100 °C, and the depth of the oxidation damage zone is directly related to the pore size; the smaller is the pore size, the lower is the oxidation induced damage. In addition, these studies have clearly shown that internal oxidation also generates tensile residual stresses which affect strength properties of RBSN.

3.3. Cycling effects on mechanical properties

The SCS-0/RBSN and the SCS-6/RBSN composites were cycled 5 times between 250 and 1400 °C in nitrogen or in oxygen and were then tensile tested at room temperature. Typical tensile stress–strain curves of the as-fabricated and cycled composites are shown in Figs 9a and b. Fig. 9a shows that the stress–strain curves of SCS-0/RBSN composites both in the as-fabricated condition and after thermal cycling in nitrogen are essentially the same and are linear up to fracture; a behaviour similar to that of monolithic RBSN. The same composite cycled in oxygen also displayed linear elastic behaviour to fracture, but the ultimate strength

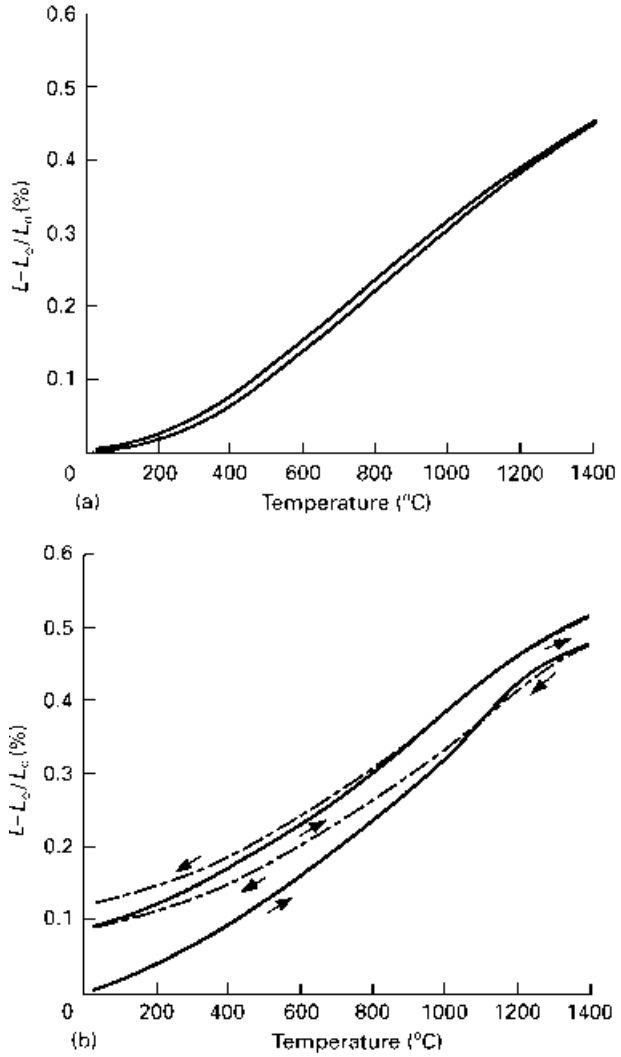

Figure 7 Effects of thermal cycling and environment on the thermal expansion curves of an unreinforced RBSN; (a) nitrogen and (b) oxygen (— 1st cycle; ——— 2nd cycle; – – – 6th cycle).

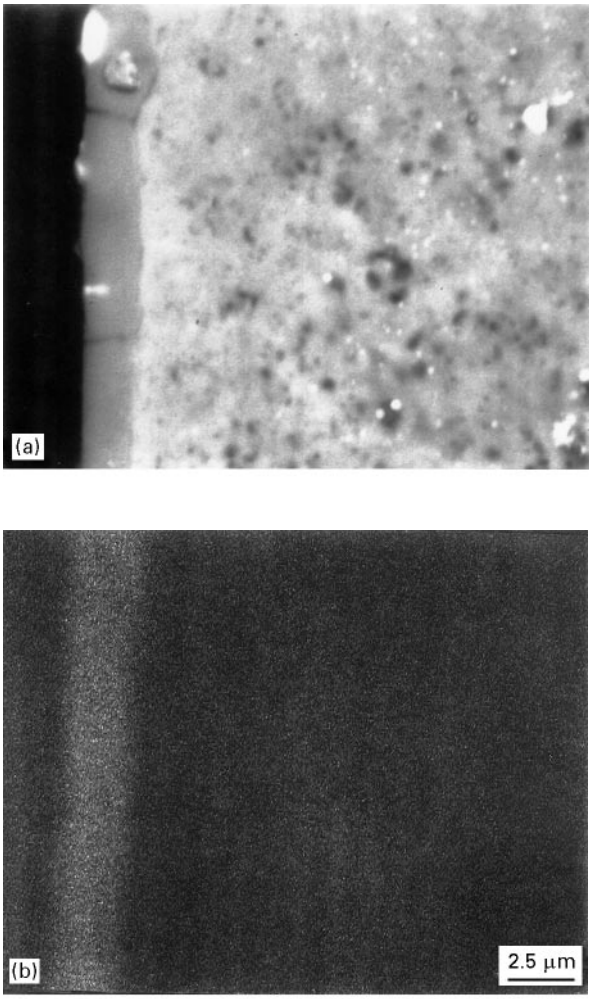

Figure 8 SEM photographs of unreinforced RBSN cycled in oxygen showing formation of oxide layer on the external surface. (a) Back scattered image and (b) oxygen X-ray image.

TABLE II Specimen length increase with thermal cycles for SiC/RBSN composites and RBSN matrix in oxygen

Material	Orientation of fibres to measurement	Length increase with cycle (%)		
		1st	2nd	3rd
SCS-6/RBSN	Parallel	0.10	0.00	0.0
SCS-6/RBSN	Normal	0.21	0.00	0.0
SCS-0/RBSN	Parallel	0.08	0.02	0.0
SCS-0/RBSN	Normal	0.10	0.0	0.0
RBSN	None	0.08	0.0	0.0

was lower than that of a nitrogen cycled or as-fabricated composite. On the other hand, the stress–strain curves of the as-fabricated, and nitrogen cycled SCS-6/RBSN composites showed two linear regions separated by a non-linear region, but those of the same composites cycled in oxygen displayed only one linear region and considerable loss in strength.

Room-temperature property data measured from the tensile stress–strain curves for the as-fabricated and cycled SCS-6/RBSN composites are summarized in Table III. The SCS-0/RBSN composites showed no strain capability beyond matrix fracture and low strength which degraded further after cycling; their property data are not included in Table III. Reported data in Table III indicate that the as-fabricated strength properties of the SCS-6/RBSN composites remained nearly the same after cycling in nitrogen, but cycling in oxygen resulted in loss of tensile properties. The first matrix fracture strength for the composites cycled in oxygen was consistently lower than that for the as-fabricated composites or for the composite cycled in nitrogen. The tensile fracture surfaces of the SCS-0/RBSN composites, whether in the as-fabricated or in the thermally cycled condition, showed brittle failure. Similar examination of the as-fabricated and nitrogen cycled SCS-6/RBSN composites showed extensive fibre pull out and a broomy fracture surface. In contrast, the SCS-6/RBSN composites cycled in oxygen exhibited essentially a brittle fracture (Fig. 10).

Elemental oxygen and carbon X-ray images of the cross-sections for the SCS-6/RBSN composites cycled in nitrogen and in oxygen are shown in Fig. 11. In nitrogen, the carbon-rich coating is stable, but in oxygen, the coating is oxidized completely. The silica layer formed on the fibre surface cracked circumferentially such that part of it was attached to the fibre and part to the matrix. Indication of carbon between the silica layers in composites cycled in oxygen is an artifact

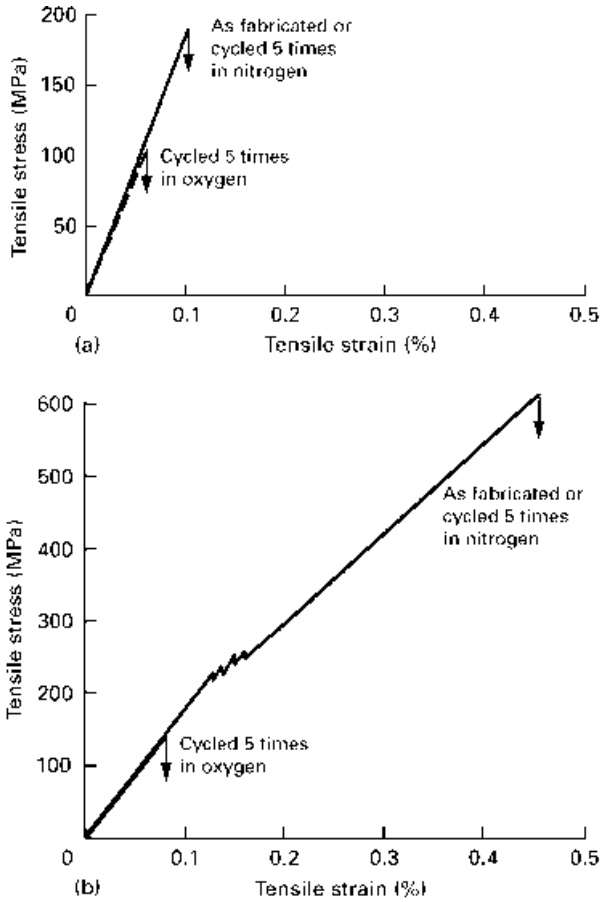

Figure 9 Representative room-temperature tensile stress–strain curves for SiC/RBSN composites in the as-fabricated condition and cycled 5 times in nitrogen and in oxygen from 25 to 1400 °C. (a) SCS-0/RBSN and (b) SCS-6/RBSN.

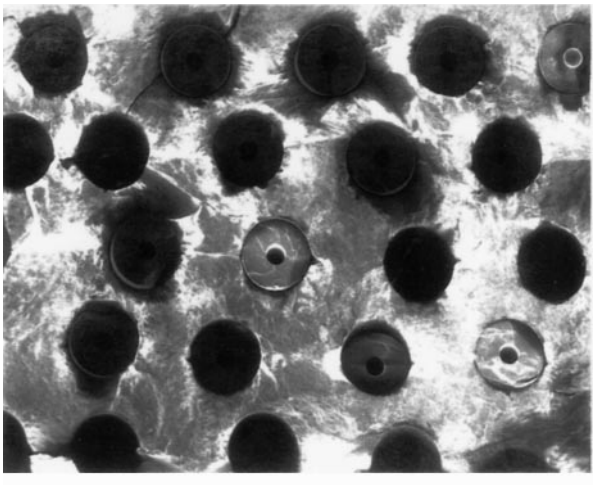

Figure 10 Tensile fracture surface of a SCS-6/RBSN composite cycled in oxygen showing brittle failure.

created by the infiltration of epoxy used in the preparation of the specimen. Based on the thermal expansion results in oxygen, the loss of the first matrix fracture strength in composites can be attributed to swelling of the RBSN matrix and redistribution of residual stresses resulting from the internal oxidation of the RBSN matrix. As discussed previously, in the as-fabricated SCS-6/RBSN composites, the SCS-6 fibres and RBSN matrix are under residual tension and compression along the fibre direction, respectively. After cycling the composites in oxygen, the fibres are under even higher tensile residual stress and the RBSN matrix is under lower compressive residual stress due to internal oxidation of the matrix. The altered residual stress pattern affects both first matrix cracking and ultimate strength.

Noticeable differences were seen in the mechanical response of the composites subjected to static and cyclic oxidation conditions. In a previous study [16] oxidation behaviour of SCS-6/RBSN composites at temperatures to 1400 °C, and their room temperature mechanical properties after 100 h static exposure in oxygen up to 1400 °C have been investigated. Results indicated loss of mechanical properties for composites exposed between 500 and 1100 °C, but those exposed to 1200 °C and above retained a greater fraction of the as-fabricated strength. In all exposure conditions the composite showed strain capability beyond matrix fracture. In contrast, the composite cycled between 25 and 1400 °C in oxygen displayed no strain capability beyond matrix fracture. In static oxidation at low temperatures, i.e. 500 to 1000 °C, oxidation of the carbon-rich coating resulted in a gap between the fibre and the matrix. Internal oxidation of RBSN matrix was prevalent between 800 and 1100 °C. Poor load transfer between the fibre and the matrix, and loss of fibre strength due to oxidation of the carbon-rich

TABLE III Room-temperature tensile properties of unidirectional SCS-6/RBSN composites ($V_f \sim 0.24$)

Room-temperature properties	As-fabricated[a] (not cycled)	After 5 cycles in nitrogen[b] 25 to 1400 °C	After 5 cycles in nitrogen[b] 25 to 1400 °C
Elastic modulus (GPa)	178 ± 16	186	173
Tensile strength (MPa)			
First matrix	220 ± 24	213	138
Ultimate	680 ± 62	551	138
Strain to failure (%)			
First matrix	0.12	0.11	0.08
Ultimate	0.45	0.40	0.08

[a] Average of 5 specimens.
[b] Average of 3 specimens.

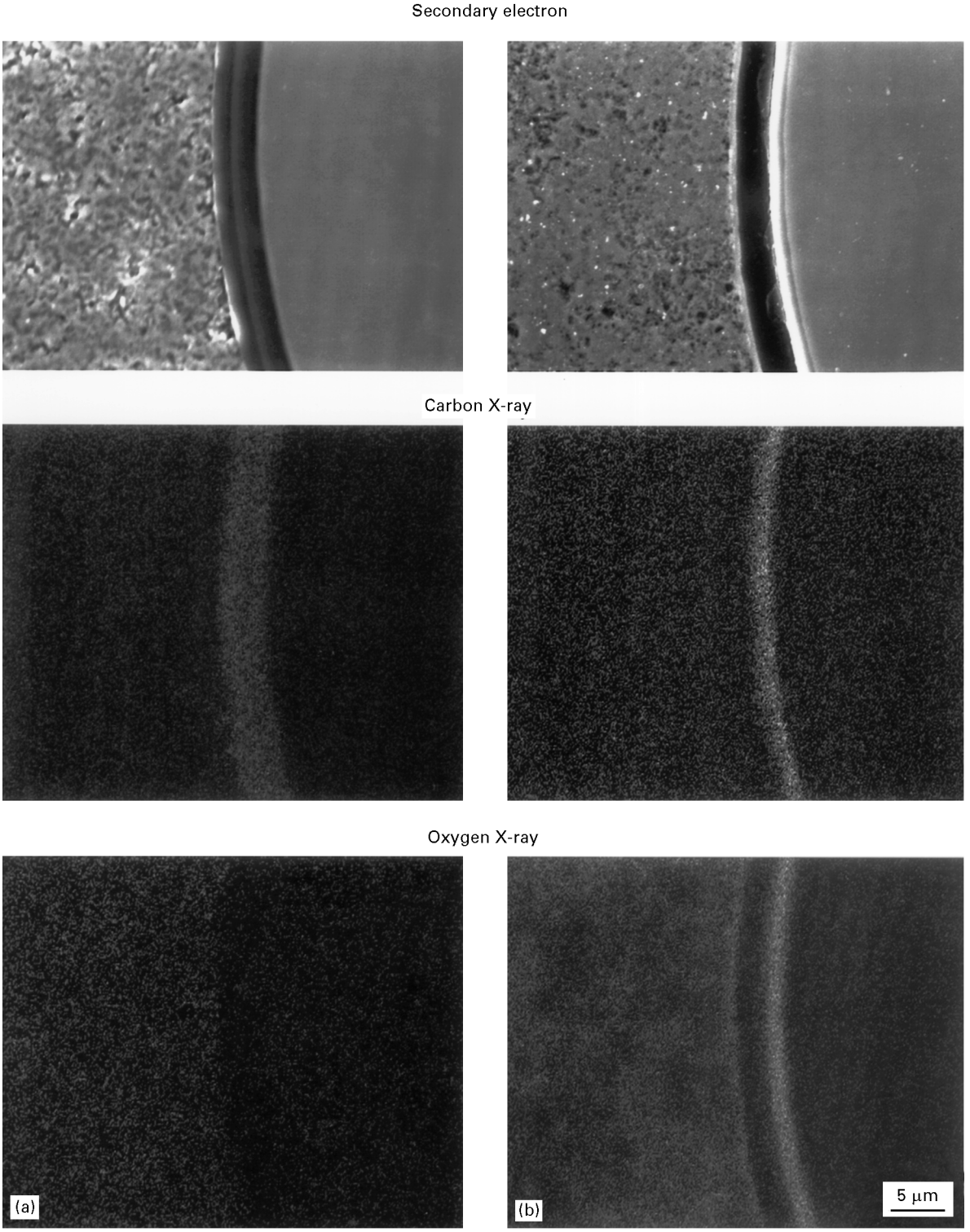

Figure 11 Elemental X-ray photographs of the cross-sections of SCS-6/RBSN composites showing oxidation of carbon-rich interface coating: (a) as-fabricated (uncycled) and (b) cycled 5 times in oxygen between 250 and 1400 °C.

coating contributed to the loss of mechanical properties of the composite. On the other hand, in static exposure at temperatures exceeding 1200 °C, formation of silica on the surface of the specimens rapidly restricted the oxidation to the surface and also reduced the oxidation of the carbon-rich coating on the fibres, fibre degradation and internal oxidation of the matrix. Thus a greater fraction of as-fabricated mechanical properties was retained.

In cyclic oxidation, even though a silica layer is formed at the surface during the heating cycle, this silica layer cracked upon cooling to room temperature, similar to the case of unreinforced RBSN cycled in oxygen as shown in Fig. 9. This cracking permitted entry of oxygen during the second heating cycle. In addition, a gap formed at the interface due to differential shrinkage of the fibre and the matrix during cycling also caused oxidation of the interface carbon coating through the exposed ends of the fibres which promoted a stronger bond between the fibre and the matrix. Oxidation of the fibres' surface coating coupled with formation of a stronger bond between

the SiC fibre and the RBSN matrix, resulted in a loss of strain capability of the fibre and brittle behaviour. In addition internal oxidation of the matrix resulted in volume expansion. This study clearly indicates that cyclic oxidation of SCS-6/RBSN composites between 25 and 1400 °C results in significant loss in mechanical properties compared with static oxidation of the same composite at 1400 °C for 100 h.

4. Summary of results

Thermal expansion properties of unidirectional SCS-0 and SCS-6 fibre-reinforced RBSN composites were determined from 250 to 1400 °C. The measured data compared well with the values predicted from a rule-of-mixtures model. The effect of cycling in an inert and in an oxidizing environment on thermal expansion curves and on tensile properties of the SCS-0 strongly- and SCS-6 weakly-bonded SiC/RBSN composites showed important results as follows:

1. The rule-of-mixtures model can be used to predict thermal expansions parallel and normal to the fibre direction for the SiC/RBSN composites for up to 700 °C.
2. Fibre/matrix bonding shows a strong influence on thermal expansion parallel to the fibre and no or minimal influence on thermal expansion transverse to the fibres.
3. Thermal cycling of the SCS-0/RBSN or the SCS-6/RBSN composites in nitrogen caused no significant change in length or room-temperature tensile properties from the as-fabricated condition.
4. In an oxygen environment, thermal cycling of the SCS-6/RBSN composites resulted in volume expansion and loss of tensile properties and catastrophic failure.
5. Similar studies on monolithic RBSN suggests that internal oxidation of the RBSN matrix is responsible for the volume expansion. Oxidation of the carbon-rich coating and formation of silica which promoted degradation in fibre strength appear to explain the poor mechanical properties of oxygen cycled composites.

5. Conclusions

Thermal expansion SiC/RBSN composites can be reasonably predicted by rule-of-mixture models. Thermal cycling of the composite in nitrogen has no effect on composite dimensions or mechanical performance, but thermal cycling in oxygen causes volume expansion and degradation of mechanical properties due to oxidation of matrix and fibre/matrix interface coating, resulting in increased tensile stress on fibre and loss of fibre strength. Possible approaches to resolve the cyclic oxidation problems are by (i) sealing the external surfaces of the composite with denser layers of CVD SiC or Si_3N_4, (ii) by infiltrating the composite with SiC or Si_3N_4 by CVI or polymer pyrolysis methods, or (iii) by densifying the matrix by HIPing.

References

1. C. A. ANDERSON, P. BORRON-ANTOLIN, A. S. FAREED and G. H. SCHIROKY, in "Whisker- and Fiber-Toughened Ceramics" edited by R. A. Bradley, D. E. Clark, D. C. Larsen, and J. O. Stiegler (American Society for Metals International, Metals Park, OH, 1988) p. 209.
2. R. T. BHATT and R. E. PHILLIPS, *J. Compos. Technol. Res.* **12** (1990) 13.
3. W. FOULDS, J. F. LECOSTAOUEC, C. LANDRY, S. DIPIETRO and T. VASILOS, *Ceram. Eng. Sci. Proc.* **10** (1989) 1083.
4. P. I. LIMICQ, G. A. BERNHART, M. M. DAUCHIER and J. G. MACE, *Amer. Cer. Soc. Bull.* **65** (1986) 336.
5. K. M. PREWO and J. J. BRENNAN, *J. Mater. Sci.* **15** (1980) 463.
6. R. T. BHATT, in "Whisker- and Fiber-Toughened Ceramics", edited by R. A. Bradley, D. E. Clark, D. C. Larsen, and J. O. Stiegler (American Society for Materials International, Metals Park, OH, 1988) p. 209.
7. P. PIROUZ, G. MORSCHER and J. CHANG, in "Surface and Interfaces of Ceramic Materials" edited by L. C. Dufour (Kluwer Academic Publishers, Dordrecht, 1989) p. 737.
8. R. T. BHATT, US Patent No. 4689188 (1987).
9. J. ELDRIDGE, private communication.
10. R. A. SCHAPERY, *J. Compos. Mater.* **2** (1968) 380.
11. P. S. TURNER, *J. Res. Nat. Bur. Stand. (US)* **37** (1946) 239.
12. J. A. DICARLO, in "Whisker- and Fiber-Toughened Ceramics", edited by R. A. Bradley, D. E. Clark, D. C. Larsen, and J. O. Stiegler (American Society for Materials International, Metals Park, OH, 1988) p. 1.
13. W. S. COBLENZ, *J. Amer. Ceram. Soc.* **58** (1975) 530.
14. F. PORZ and F. THUMMLER, *J. Mater. Sci.* **19** (1984) 1283.
15. A. G. EVANS and R. W. DAVIDGE, *ibid.* **5** (1970) 314.
16. R. T. BHATT, *J. Amer. Ceram. Soc.* **75** (1992) 406.

Received 20 November 1995
and accepted 17 September 1996